

PHY6480 | Research Project in Physics

Drift-Diffusion Simulations of Wide Bandgap Perovskite Solar Cells

Submitted: 23 February 2024**Dinesh Behera^{a)}**

AFFILIATIONS

Department of Physics and Astronomy, The University of Sheffield, S3 7RH, United Kingdom

^{a)}Author to whom correspondence should be addressed: dbehera1@sheffield.ac.uk

ABSTRACT

In the face of pressing global challenges like climate change, the pursuit of efficient renewable energy sources becomes paramount. Tandem and multijunction photovoltaics stand out as innovative approaches as these couple two or more solar cells together to convert a wider range of the available solar spectrum into electricity. While single-junction solar cells can achieve efficiencies of ~26% (for silicon), tandem and multijunction devices can achieve efficiencies of >40%. Perovskite solar cells are desirable for tandem applications as their tunable bandgaps allow them to be used in various tandem applications (e.g. silicon, organics, CIGS, and perovskites) and they are cost-effective. The research project outlined in this review takes a computational approach, utilising drift-diffusion simulations to model solar cells based on a recently developed halide-segregation-suppressed wide-bandgap perovskite. To explore its multijunction applications, the study aims to unravel the nuanced interplay of different device parameters influencing solar cell performance. Through this comprehensive analysis, the goal is to pinpoint the specific combination of parameters that contributed to the record efficiency achieved in the recently reported perovskite solar cell.

INTRODUCTION

Why Solar Energy?

In the contemporary world, our reliance on electrical energy to drive industries, power homes, and fuel technological advancements has surged to an approximate annual demand of 25500 terawatts-hour (TWh), as reported by the International Energy Agency's annual energy reports.¹

Despite this soaring demand, a predominant share (around 62%) is still fulfilled through the combustion of fossil fuels, encompassing oil, coal, and natural gas. In comparison, renewables currently account for only about 25% of the global energy supply.^{2,3} Notably, solar radiation, with a spectral intensity of 1000 watts per square meter (W/m^2) falling on Earth's landmass, constitutes a staggering incoming power of 26,000 TW.⁴ However, despite this huge incoming power from the sun, the contribution of solar radiation harvesting to meet energy demand stands at a mere fraction, representing just around 3-5% of the renewable energy share.^{2,3}

This inconsistency between the abundant solar resource available and its limited utilisation underscores the untapped potential and challenges in fully harnessing solar energy for a more sustainable and diversified energy portfolio. As we strive to address the environmental impact of conventional energy sources, unlocking the full potential of solar radiation harvesting through photovoltaics (PV) becomes imperative for a cleaner, more resilient energy future. Advances in solar cell technologies through enhancing efficiency and stability, and lowering the cost of production are essential to bridge this gap, lower the cost of solar electricity (\$/kWh), and transition towards a more PV-centric energy mix.

Detailed Balance Limit on Efficiency

In photovoltaics, theoretical detailed balance calculations uncover the fundamental limitations of single junction solar cells, indicating a maximum achievable power conversion efficiency of 33.7%. This efficiency peak is anticipated when the bandgap energy reaches approximately 1.34 eV.⁵ This limit on the PCE arises due to:-

- (a) transmission (photon energy $<$ bandgap) and thermalisation (photon energy $>$ bandgap) processes, which affect the short circuit current (J_{SC}), account for about a minimum of 33% of the total PCE losses;
- (b) non-radiative recombination losses which give rise to higher open circuit voltage deficit ($V_{\text{OC, deficit}} = E_g/e - V_{\text{OC}}$), account for about a minimum of 20% of the total PCE losses;
- (c) parasitic resistance (series and shunt resistances) losses, which affect the fill factor (FF), account for about a minimum of 13% of the total PCE losses.⁶

Nevertheless, a strategy to surpass the PCE limitation involves mitigating short-circuit current density (J_{SC}) losses and increasing the open-circuit voltage (V_{OC}) by incorporating multiple solar cells with their light-absorbing layers having complementary bandgaps. These devices are tandem solar cells (two junctions - 2J) and multijunction solar cells (3J or more). The tandem solar cell devices are available in two architectures, as shown in FIG. 1, one is a 4-terminal device (stacked tandem architecture) and the other is a 2-terminal device (monolithic tandem architecture).

The 4-terminal device extracts the most power theoretically (a PCE of about 55% for a 2J device)⁶, however, the problem is that their deployment is expensive and more challenging as

these need double combiner boxes, power distribution cabinets, and inverters to maintain the efficiency boost, which is difficult to do in practice. Hence, 2-terminal devices are preferred where only the V_{OC} is enhanced. In such 2-terminal tandem and multijunction devices, V_{OC} is given by the sum of the V_{OC} of the subcells in the stack. Hence, the multijunction devices' power conversion efficiency is given as:-

$$PCE = \frac{\sum_{i=1}^n V_{OC}^i * J_{SC}^{*FF}}{P_{in}} \text{ [Equation 1].}^6$$

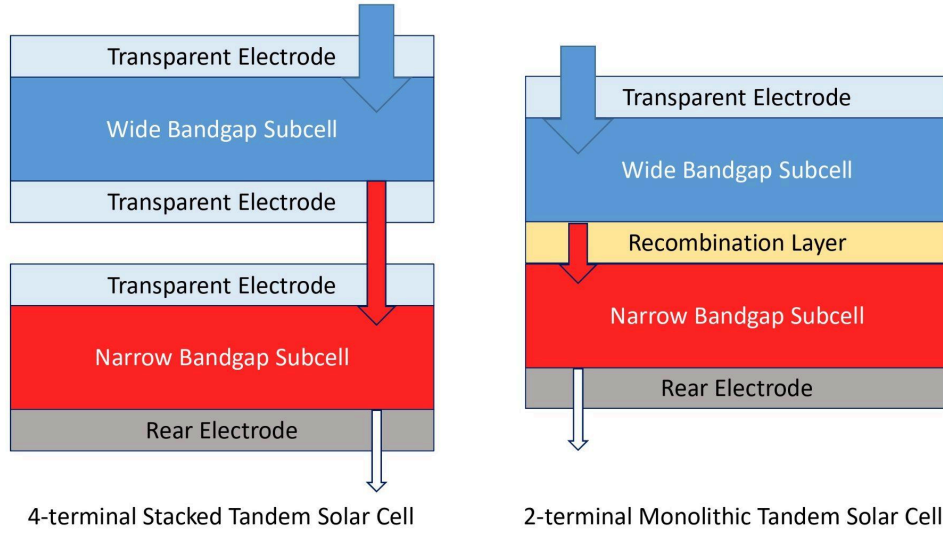


FIG. 1. Tandem solar cell architectures: stacked 4-terminal architecture (left) and monolithic 2-terminal architecture (right); wide bandgap subcell absorbing the high energy photons (denoted in blue), narrow bandgap subcell absorbing the low energy photons (denoted in red), and the transmitted/unabsorbed light (denoted in white).

In tandem and multijunction architectures, one of the primary obstacles lies in achieving compatibility among materials characterised by distinct bandgaps and electronic properties. The seamless integration of these materials is pivotal for facilitating efficient charge carrier transport and collection within the stacked layers.⁶ Simultaneously, the optical design demands meticulous attention to detail, necessitating transparent and highly efficient non-absorber layers that permit optimal light penetration to the absorber layers while mitigating losses.^{6,7} Current matching, a critical aspect, entails balancing current outputs from individual subcells to prevent energy losses and ensure the tandem cell operates at peak efficiency.^{6,8} Furthermore, perovskite tandem solar cells face stability concerns arising from integrating diverse materials, necessitating measures to safeguard against degradation and ensure long-term reliability.⁸ The intricacy of fabrication processes adds another layer of complexity, and cost considerations pose a challenge to achieving competitiveness with traditional single-junction solar cell technologies.⁶⁻⁸ Addressing these

challenges is imperative for harnessing the full potential of tandem solar cells and advancing their integration into mainstream photovoltaic applications. Ongoing research endeavors focus on materials innovation, improved fabrication techniques, and enhanced device engineering to overcome these hurdles and propel tandem solar cells toward commercial viability.

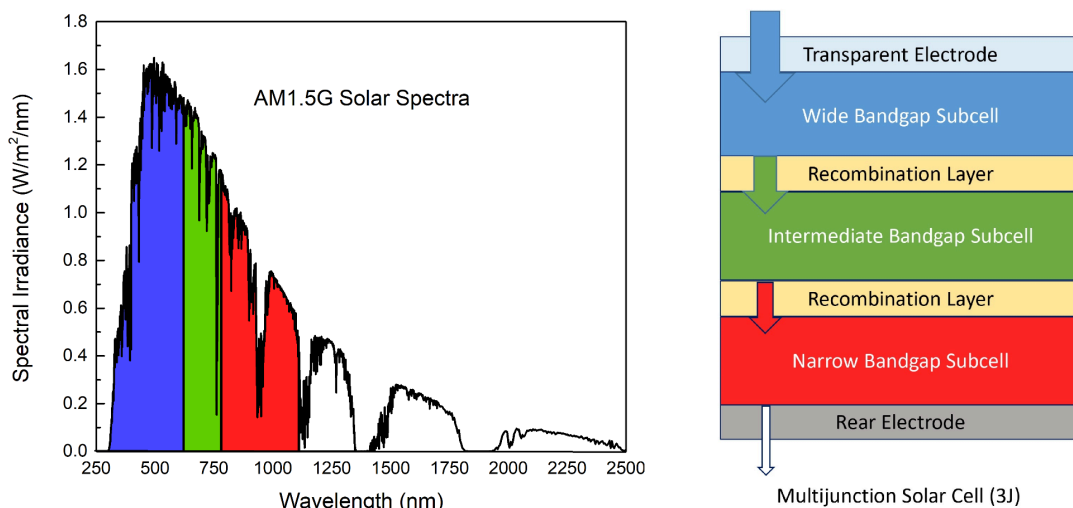


FIG. 2. The terrestrial solar irradiance absorbed by a multijunction solar cell (3J): wide bandgap subcell absorbing the high energy photons (denoted in blue), intermediate bandgap subcell absorbing the intermediate energy photons (denoted in green), narrow bandgap subcell absorbing the low energy photons (denoted in red), and the transmitted/unabsorbed light (denoted in white).

Current Research Focus

The maximum PCE achievable by multijunction solar cells as predicted by the detailed balance limit calculations is about 65%.^{9,10} As of current state of the art, multijunction solar cells based on III-V semiconductors like GaAs and GaInP have demonstrated impressive potential in 2J, 3J, and 4J configurations, achieving notable PCEs of approximately 31%, 38%, and 39%, respectively, under standard terrestrial conditions.¹¹ Despite their high performance, III-V multi-junction solar cell technologies have drawbacks, including rigidity, thickness (80 to 200 μm), weight (power generated per gram: 0.4-0.8 $\text{W}\cdot\text{g}^{-1}$), and complex fabrication processes.^{12,13} Research is now focused on cost-effective alternatives, particularly perovskites-based tandem and multijunction. The perovskite/silicon and perovskite/perovskite tandem solar cells have currently reached PCEs of about 34% and 29%, respectively.¹¹ These advancements underscore the potential of perovskite-based tandem configurations as a promising avenue for pushing the boundaries of solar cell efficiency to surpass the III-V multijunction devices. However, perovskites lag in terms of stability to illumination, temperature, and moisture; which have not let perovskite solar cells be commercially viable. Ongoing research focuses on improving the operational stability of perovskites by various approaches like additive engineering, solvent engineering, compositional optimisation, interface engineering, device engineering, surface passivation, and encapsulation engineering.¹⁴ These concerted efforts aim to enhance the

operational stability of perovskites, paving the way for their integration into commercially viable PV technologies and establishing them as competitive alternatives to conventional technologies.

BACKGROUND

Tandem and Multijunction Perovskite Photovoltaics

Perovskites, characterised by their ABX_3 crystal structure, exhibit significant promise in tandem and multijunction solar cell devices due to their broad range tunable bandgap, low-cost solution-based fabrication, high absorption coefficient ($\geq 10^5 \text{ cm}^{-1}$), high efficiency, high tolerance to defects, high specific power ($23 \text{ W} \cdot \text{g}^{-1}$), and exceptional radiation tolerance.^{15–18} These appealing attributes position perovskites as attractive absorbers not only for terrestrial applications but also for space applications.

By selecting and combining specific components—A = (Cs, MA or FA), B = (Sn or Pb), and X = (I, Br or Cl)—the bandgap of perovskites can be finely tuned across a range from 1.2 eV to 3.5 eV.¹⁵ This tunability is particularly crucial for their effectiveness in tandem and multijunction solar cells which makes perovskites to be used as absorbers from top subcell to bottom subcell resulting in all-perovskite multijunction devices. Research by Hörantner et al. has underscored that perovskite-based tandem and multijunction devices hold the potential to surpass the performance records set by III-V tandem and multijunction solar cells.¹⁹

To surpass the III-V multijunction devices, Hörantner et al. highlighted the need for specific top subcell optoelectronic qualities to enhance the efficiency of tandem and multijunction device stacks. The first imperative is the development of a top perovskite subcell with a bandgap of 1.8 eV and a V_{OC} of 1.4 V for the success of all-perovskite tandem cells. Additionally, the realisation of a 2.0 eV wide-bandgap perovskite solar cell with a $V_{OC} > 1.5 \text{ V}$ is deemed essential for triple-junction architectures.¹⁹

The narrow bandgap (NBG) absorbers for bottom cells in tandem and multijunction devices are well-established as wafer-based crystalline silicon (1.12 eV bandgap), and thin-film-based CIGS ($\text{CuIn}_{1-x}\text{Ga}_x\text{Se}_2$, varying x can tune the bandgap to as low as 1.0 eV).^{20,21} However, crystalline silicon wafers are thick, rigid, and cost ineffective; and, the CIGS are thin but are heavy ($3 \text{ W} \cdot \text{g}^{-1}$) as compared to perovskites.¹³ For all-perovskites-based tandem and multijunction devices, mixed Sn/Pb perovskites as bottom subcell absorbers have already proven to possess the potential to reach near their detailed balance theoretical limit.²² The intermediate bandgap (typically 1.6 eV) absorbers in the multijunction devices are plenty and well-established as the various mixed-cation and mixed-halide-based perovskites. Lead-based I/Br mixed-halide perovskites ($\text{APb}(\text{I}_{1-x}\text{Br}_x)_3$), on increasing x, exhibit bandgaps ranging from 1.5 to 2.4 eV.^{15,23} Hence, based on the bandgap range, these mixed-halide perovskites make the appropriate wide bandgap (WBG) absorbers in tandem and multijunction devices.

Implementation Issues of Perovskite Multijunction

However, the quest for suitable bandgap faces complexities in terms of unstable compositions, and thereby the WBG absorbers have yet to achieve comparable success in PCE as their bottom cell counterparts. The low PCEs of WBG solar cells, which further decreased after continuous operation, were for many years attributed to the V_{OC} losses arising from light-induced phase segregation or halide segregation (also known as the Hoke effect).²⁴ Halide segregation is prominent after the Br content reaches 20% in mixed-halide perovskite films, resulting in the development of iodide-rich and bromide-rich phases. These iodide-rich phases exhibit lower bandgaps than the surrounding material, hence limiting the maximum V_{OC} of the solar cell to 1.2 V.^{23,24} As stated above, a $V_{OC} > 1.5$ V is essential for realising the full potential of WBG perovskite solar cells, however, is not achievable due to halide segregation.

The studies by Mahesh et al. using optical modelling based on detailed balance calculations and Fourier transform photocurrent spectroscopy (FTPS) have revealed that the prime reason behind the V_{OC} losses in WBG mixed-halide perovskites is their optoelectronic quality, i.e. a significant obstacle revolves around trap-assisted non-radiative-recombination and interfacial non-radiative recombination occurring at the interface between perovskite absorber and charge extraction layers.²³ The mitigation of trap density in mixed-halide perovskites not only serves to optimize the initial V_{OC} but also holds the potential to alleviate issues related to halide segregation, given the observed positive correlation between higher trap densities and the occurrence of halide segregation. Efforts are underway to address this issue, and while progress has been made in mitigating the problem, there is still room for improvements in the case of 2.0 eV bandgap perovskites as these have the potential to achieve a $V_{OC} \sim 1.6$ V theoretically while the maximum these have reached is 1.4 V.^{25,26}

Novel Halide-Segregation-Stable Wide Bandgap Perovskite

Yu et al. have shown that inorganic perovskites showcase higher thermal and light illumination stabilities than hybrid organic-inorganic perovskites. Cs-based mixed halide perovskites, which feature smaller A-site cations and higher iodide anion content, exhibit greater lattice distortion and superior stability under illumination compared to hybrid organic-inorganic perovskites.²⁷ However, though 2.0 eV bandgap Cs-based mixed-halide perovskites (e.g. $\text{CsPbI}_{1.4}\text{Br}_{1.6}$) are suggested to have improved thermal and illumination stability to 2.0 eV hybrid perovskites, as the top cell absorber in multijunction devices, these still face the issue of phase segregation to some extent when exposed to light.²⁸

The latest advancements in mitigating halide segregation involve innovative compositional engineering strategies, as evidenced by the work of Wang et al. Specifically, they explored the suppression of halide segregation by introducing Rb doping into Cs-based inorganic I/Br mixed-halide perovskites, $\text{Rb}_x\text{Cs}_{1-x}\text{Pb}(\text{I}_{1-y}\text{Br}_y)_3$.²⁸ Their findings propose that the deliberate

manipulation of perovskite lattice distortion through compositional engineering plays a pivotal role in creating an ion migration barrier. This barrier, in turn, contributes to effectively suppressing phase segregation. Further, they used this novel perovskite composition to build 2.0 eV WBG single-junction solar cells and employed those to build triple-junction solar cells. To show the superior halide-segregation suppression of their novel Rb/Cs mixed-cation mixed-halide perovskite, they compared it with the Cs-based mixed-halide perovskite. They found that the Cs-based mixed-halide perovskite solar cell starts phase segregation, thereby losing PCE within an hour, while the novel Rb/Cs mixed-cation mixed-halide perovskite remains stable for 450 hours of operation. Furthermore, the triple junction solar cell with an Rb/Cs mixed-cation mixed-halide perovskite-based top subcell also showed 80% PCE retention till 420 hours of continuous operation, with an excellent V_{OC} of 3.2 V, however, with a low J_{SC} , the overall PCE achieved is 24.3%. The highest PCE (25.1%) recorded for all-perovskite triple-junction solar cells with Cs/FA mixed-cation mixed-halide perovskite as the top subcell absorber is from the same research group as Wang et al., however, this PCE sustained 80% of its initial PCE for 200 hours of continuous operation. Hence the Rb/Cs mixed-cation mixed-halide perovskite is by far the most halide-segregation-stable perovskite reported.^{26,28}

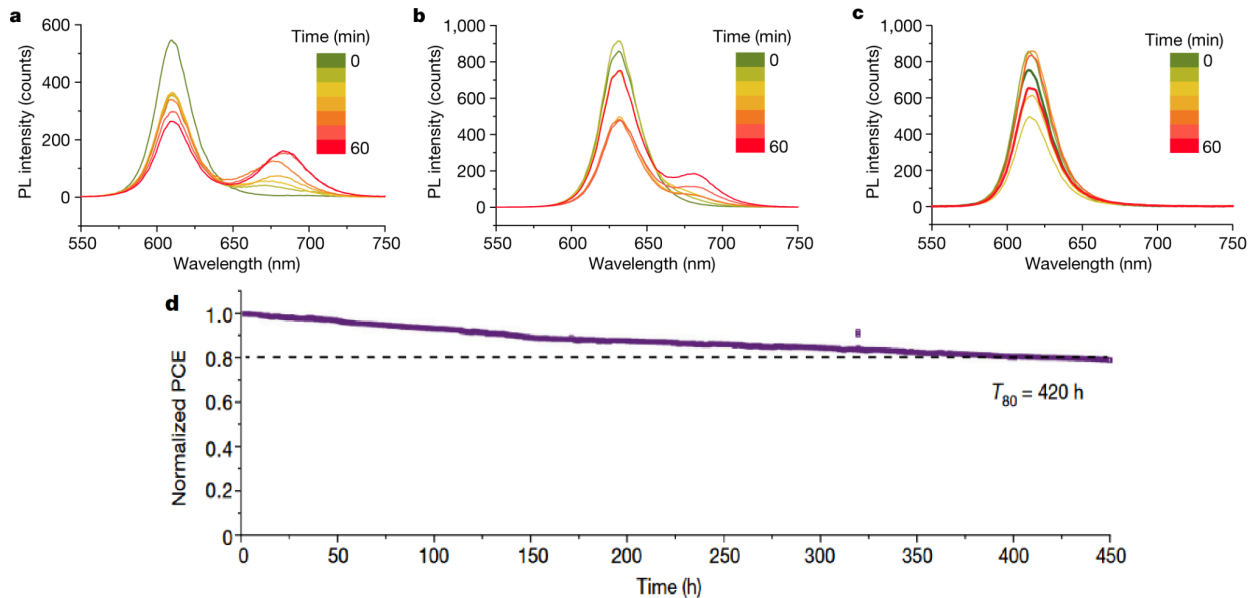


FIG. 3. PL spectra showing halide segregation in 2.0 eV perovskites, (a) CsPbI_{1.4}Br_{1.6} and (b) CsPbI_{1.75}Br_{1.25}; and the halide segregation stable (c) Rb_{0.15}Cs_{0.85}PbI_{1.75}Br_{1.25}; (d) shows the high stability of the solar cell device based on Rb_{0.15}Cs_{0.85}PbI_{1.75}Br_{1.25} as a result of suppressed halide segregation. FIG.3. (a) to (d) adapted from ref. ²⁸ (Wang et al.)

Drift-Diffusion Simulations

The fundamental device equations governing the behavior of semiconductor devices, particularly solar cells, are critical for understanding their operation. Poisson's equation establishes the

relationship between electric field strength (E), charge density (ρ), and material permittivity (ϵ). In semiconductors, the net charge density (ρ) is the summation of hole density (p), electron density (n), acceptor atom density (N_A), and donor atom density (N_D), given as:-

$$\frac{dE}{dx} = \frac{\rho}{\epsilon} = \frac{q}{\epsilon} * (p(x) - n(x) - N_A^- + N_D^+) \text{ [Equation 2].}^{29-31}$$

The transport equations describe carrier movement, involving electron current density (J_n), hole current density (J_p), electron mobility (μ_n), hole mobility (μ_p), electron diffusivity (D_n), and hole diffusivity (D_p). These equations incorporate drift and diffusion components, reflecting the flow of carriers under the influence of an electric field and a concentration gradient, respectively, and are given as:-

$$J_n = (n * e * \mu_n * E) + (e * D_n * \frac{dn}{dx}) \text{ [Equation 3]}$$

$$J_p = (p * e * \mu_p * E) - (e * D_p * \frac{dp}{dx}) \text{ [Equation 4].}^{29-31}$$

Continuity equations, crucial for "bookkeeping," track carriers in terms of current, generation rate, and recombination rate. Under steady-state conditions in solar cells, where transients are zero, the carrier concentrations remain constant over time. The continuity equations ensure that carriers are appropriately accounted for, considering generation rates (G) and recombination rates (R), and are given as:-

$$\frac{1}{e} * \frac{dJ_n}{dx} = R - G \text{ [Equation 5]}$$

$$\frac{1}{e} * \frac{dJ_p}{dx} = - (R - G) \text{ [Equation 6].}^{29-31}$$

The general conditions and relationships among these equations provide a comprehensive understanding of the complex interplay of charge carriers within a semiconductor device. As all of the above differential equations are coupled, the analytical solutions are challenging, but these can be readily solved by numerical approaches facilitated by various device simulators for efficient analysis and optimisation. Such a photovoltaic device numerical simulator tool based on the above 1D device equations is the SCAPS-1D, which was developed at the Department of Electronics and Information Systems (ELIS) of the University of Gent, Belgium.^{29,31}

Significance, Context, and Implications of this Research

This research project will delve into the intricacies of the device physics governing the operation of the novel 2.0 eV bandgap solar cell, where halide segregation has been effectively suppressed through the incorporation of Rb in Cs-based mixed-halide perovskites. The investigation aims to establish correlations between various device parameters and power conversion efficiency, offering insights for refining the device stack to optimise the performance of this innovative

wide-bandgap solar cell. Key aspects under scrutiny include layer thickness, the influence of different transport layers (TL), doping strategies for TLs, and the density of trap states/defects at both bulk and absorber/TL interfaces. The study employs the SCAPS-1D simulator for a comprehensive analysis. By concentrating on these device parameters, this research sets the stage for developing efficient and stable top perovskite subcells, paving the way for their integration into stable and efficient all-perovskite multijunction solar cell devices.

CONCLUSION

The implementation and commercialisation of all-perovskite multijunction solar cells and perovskite solar cells, in general, are hindered by their operational stability as perovskites are quite unstable to light, temperature, and moisture. The groundbreaking wide-bandgap perovskite, $\text{Rb}_{0.15}\text{Cs}_{0.85}\text{PbI}_{1.75}\text{Br}_{1.25}$, introduced by Wang et al., emerges as the optimal choice for the top subcell in all-perovskite multijunction solar cells, showcasing remarkable efficiency and robust stability against halide segregation. This novel inorganic perovskite material holds the potential to replace conventional inorganic wide-bandgap perovskites in multijunction applications, both on Earth and in extraterrestrial conditions. Although the all-perovskite multijunction device, fortified with the halide segregation-suppressed top cell absorber, excels in stability, it faces efficiency challenges when compared to III-V multijunction solar cell technologies. The III-V semiconductors, while sophisticated and robust, are hindered by their manufacturing intricacies. This is in stark contrast to the lightweight, cost-effective, and versatile nature of perovskites, making them ideally suited for terrestrial and space applications. However, unlocking the full potential of all-perovskite multijunction solar cells requires meticulous device-specific research. This entails studying their device physics for optimising efficiencies. In the current landscape of photovoltaics, there is a substantial need for more cost-effective solar cell technologies and all-perovskite multijunction solar cells emerge as a promising candidate, offering a bright future.

ACKNOWLEDGEMENTS

The author would like to express their sincere gratitude to Dr. Alex Ramadan for her invaluable support and supervision during the research project of the MSc in Solar Cell Technology programme (2023-24) at the Department of Physics and Astronomy, The University of Sheffield. Her guidance and expertise have been instrumental in the successful completion of this literature review. The author also acknowledges the Department of Physics and Astronomy for providing the necessary resources and facilities for conducting the literature review.

REFERENCES

- ¹“Electricity consumption – Electricity Information: Overview – Analysis,” IEA, (n.d.).
- ² F.J.M.M. Nijse, J.-F. Mercure, N. Ameli, F. Larosa, S. Kothari, J. Rickman, P. Vercoolen, and H. Pollitt, “The momentum of the solar energy transition,” *Nat. Commun.* **14**(1), 6542 (2023).
- ³ D. Zhang, C. Rong, T. Ahmad, H. Xie, H. Zhu, X. Li, and T. Wu, “Review and outlook of global

energy use under the impact of COVID-19," *Eng. Rep.* **5**(3), e12584 (2023).

⁴ D. Archer, *Global Warming: Understanding the Forecast* (John Wiley & Sons, 2011).

⁵ W. Shockley, and H.J. Queisser, "Detailed Balance Limit of Efficiency of p-n Junction Solar Cells," *J. Appl. Phys.* **32**(3), 510–519 (2004).

⁶ J.A. Nelson, *The Physics Of Solar Cells* (World Scientific Publishing Company, 2003).

⁷ M. Yamaguchi, F. Dimroth, J.F. Geisz, and N.J. Ekins-Daukes, "Multi-junction solar cells paving the way for super high-efficiency," *J. Appl. Phys.* **129**(24), 240901 (2021).

⁸ T. Leijtens, K.A. Bush, R. Prasanna, and M.D. McGehee, "Opportunities and challenges for tandem solar cells using metal halide perovskite semiconductors," *Nat. Energy* **3**(10), 828–838 (2018).

⁹ I.M. Peters, C.D. Rodríguez Gallegos, L. Lüer, J.A. Hauch, and C.J. Brabec, "Practical limits of multijunction solar cells," *Prog. Photovolt. Res. Appl.* **31**(10), 1006–1015 (2023).

¹⁰ A.D. Vos, "Detailed balance limit of the efficiency of tandem solar cells," *J. Phys. Appl. Phys.* **13**(5), 839 (1980).

¹¹ M.A. Green, E.D. Dunlop, M. Yoshita, N. Kopidakis, K. Bothe, G. Siefer, and X. Hao, "Solar cell efficiency tables (version 62)," *Prog. Photovolt. Res. Appl.* **31**(7), 651–663 (2023).

¹² J. Li, A. Aierken, Y. Liu, Y. Zhuang, X. Yang, J.H. Mo, R.K. Fan, Q.Y. Chen, S.Y. Zhang, Y.M. Huang, and Q. Zhang, "A Brief Review of High Efficiency III-V Solar Cells for Space Application," *Front. Phys.* **8**, (2021).

¹³ R. Verduci, V. Romano, G. Brunetti, N. Yaghoobi Nia, A. Di Carlo, G. D'Angelo, and C. Ciminelli, "Solar Energy in Space Applications: Review and Technology Perspectives," *Adv. Energy Mater.* **12**(29), 2200125 (2022).

¹⁴ H. Zhu, S. Teale, M.N. Lintangpradipto, S. Mahesh, B. Chen, M.D. McGehee, E.H. Sargent, and O.M. Bakr, "Long-term operating stability in perovskite photovoltaics," *Nat. Rev. Mater.* **8**(9), 569–586 (2023).

¹⁵ J. Albero, A. M. Asiri, and H. García, "Influence of the composition of hybrid perovskites on their performance in solar cells," *J. Mater. Chem. A* **4**(12), 4353–4364 (2016).

¹⁶ Y. Tu, J. Wu, G. Xu, X. Yang, R. Cai, Q. Gong, R. Zhu, and W. Huang, "Perovskite Solar Cells for Space Applications: Progress and Challenges," *Adv. Mater.* **33**(21), 2006545 (2021).

¹⁷ F. Lang, G.E. Eperon, K. Frohna, E.M. Tennyson, A. Al-Ashouri, G. Kourkafas, J. Bundesmann, A. Denker, K.G. West, L.C. Hirst, H.-C. Neitzert, and S.D. Stranks, "Proton-Radiation Tolerant All-Perovskite Multijunction Solar Cells," *Adv. Energy Mater.* **11**(41), 2102246 (2021).

¹⁸ G.E. Eperon, M.T. Hörantner, and H.J. Snaith, "Metal halide perovskite tandem and multiple-junction photovoltaics," *Nat. Rev. Chem.* **1**(12), 1–18 (2017).

¹⁹ M.T. Hörantner, T. Leijtens, M.E. Ziffer, G.E. Eperon, M.G. Christoforo, M.D. McGehee, and H.J. Snaith, "The Potential of Multijunction Perovskite Solar Cells," *ACS Energy Lett.* **2**(10), 2506–2513 (2017).

²⁰ E. Aydin, E. Ugur, B.K. Yildirim, T.G. Allen, P. Dally, A. Razzaq, F. Cao, L. Xu, B. Vishal, A. Yazmaciyan, A.A. Said, S. Zhumagali, R. Azmi, M. Babics, A. Fell, C. Xiao, and S. De Wolf, "Enhanced optoelectronic coupling for perovskite/silicon tandem solar cells," *Nature* **623**(7988), 732–738 (2023).

²¹ A. Maoucha, H. Ferhati, F. Djeflal, and F. AbdelMalek, "Highly efficient Cd-Free ZnMgO/CIGS solar cells via effective band-gap tuning strategy," *J. Comput. Electron.* **22**(3), 887–896 (2023).

²² J. Tong, Z. Song, D.H. Kim, X. Chen, C. Chen, A.F. Palmstrom, P.F. Ndione, M.O. Reese, S.P. Dunfield, O.G. Reid, J. Liu, F. Zhang, S.P. Harvey, Z. Li, S.T. Christensen, G. Teeter, D. Zhao, M.M. Al-Jassim, M.F.A.M. van Hest, M.C. Beard, S.E. Shaheen, J.J. Berry, Y. Yan, and K. Zhu,

"Carrier lifetimes of $>1\ \mu\text{s}$ in Sn-Pb perovskites enable efficient all-perovskite tandem solar cells," *Science* **364**(6439), 475–479 (2019).

²³ S. Mahesh, J.M. Ball, R.D.J. Oliver, D.P. McMeekin, P.K. Nayak, M.B. Johnston, and H.J. Snaith, "Revealing the origin of voltage loss in mixed-halide perovskite solar cells," *Energy Environ. Sci.* **13**(1), 258–267 (2020).

²⁴ E.T. Hoke, D.J. Slotcavage, E.R. Dohner, A.R. Bowring, H.I. Karunadasa, and M.D. McGehee, "Reversible photo-induced trap formation in mixed-halide hybrid perovskites for photovoltaics," *Chem. Sci.* **6**(1), 613–617 (2014).

²⁵ A.J. Ramadan, R.D.J. Oliver, M.B. Johnston, and H.J. Snaith, "Methylammonium-free wide-bandgap metal halide perovskites for tandem photovoltaics," *Nat. Rev. Mater.*, 1–17 (2023).

²⁶ J. Wang, L. Zeng, D. Zhang, A. Maxwell, H. Chen, K. Datta, A. Caiazza, W.H.M. Remmerswaal, N.R.M. Schipper, Z. Chen, K. Ho, A. Dasgupta, G. Kusch, R. Ollearo, L. Bellini, S. Hu, Z. Wang, C. Li, S. Teale, L. Grater, B. Chen, M.M. Wienk, R.A. Oliver, H.J. Snaith, R.A.J. Janssen, and E.H. Sargent, "Halide homogenization for low energy loss in 2-eV-bandgap perovskites and increased efficiency in all-perovskite triple-junction solar cells," *Nat. Energy*, 1–11 (2023).

²⁷ B. Yu, S. Tan, D. Li, and Q. Meng, "The stability of inorganic perovskite solar cells: from materials to devices," *Mater. Futur.* **2**(3), 032101 (2023).

²⁸ Z. Wang, L. Zeng, T. Zhu, H. Chen, B. Chen, D.J. Kubicki, A. Balvanz, C. Li, A. Maxwell, E. Ugur, R. dos Reis, M. Cheng, G. Yang, B. Subedi, D. Luo, J. Hu, J. Wang, S. Teale, S. Mahesh, S. Wang, S. Hu, E.D. Jung, M. Wei, S.M. Park, L. Grater, E. Aydin, Z. Song, N.J. Podraza, Z.-H. Lu, J. Huang, V.P. Dravid, S. De Wolf, Y. Yan, M. Grätzel, M.G. Kanatzidis, and E.H. Sargent, "Suppressed phase segregation for triple-junction perovskite solar cells," *Nature* **618**(7963), 74–79 (2023).

²⁹ D. Neamen, *Semiconductor Physics And Devices* (McGraw-Hill Education, 2003).

³⁰ Basore, "Numerical modeling of textured silicon solar cells using PC-1D," *Electron Devices IEEE Trans. On* **37**, 337–343 (1990).

³¹ M. Burgelman, P. Nollet, and S. Degraeve, "Modelling polycrystalline semiconductor solar cells," *Thin Solid Films* **361–362**, 527–532 (2000).